

Deformation patterns in the Van region (Eastern Turkey) and their significance for the tectonic framework

M. ALPER ŞENGÜL¹, ŞULE GÜRBOĞA^{2,✉}, İSMAİL AKKAYA³ and ALİ ÖZVAN⁴

¹Istanbul University, Institute of Natural and Applied Sciences, Department of Geological Engineering, Campus Avcılar, 34320 İstanbul, Turkey

²General Directorate of Mineral Research and Exploration, Department of Marine Researches, Dumlupınar Boulevard, no:139, 06800 Çankaya/Ankara, Turkey; ✉sule.gurboga@gmail.com

³Yüzüncü Yıl University, Institute of Natural and Applied Sciences, Department of Geophysical Engineering, Bardakçı Street, 65090 Van, Turkey

⁴Yüzüncü Yıl University, Institute of Natural and Applied Sciences, Department of Geological Engineering, Bardakçı Street, 65090 Van, Turkey

(Manuscript received September 26, 2017; accepted in revised form March 25, 2019)

Abstract: The area of investigation is located on the south-eastern shore of Lake Van in Eastern Turkey where a destructive earthquake took place on 23rd October, 2011 (Mw=7.1). Following the earthquake, different source mechanisms, deformations, and types of faulting have been suggested by different scientists. In this research, Edremit district and vicinities located on the southern side of Van have been investigated to understand the deformation pattern in a travertine (400 ka) formation on the surface, and its structural and stratigraphic relationships with the main faults under the surface by using two-dimensional (2D) Electrical Resistivity Tomography (ERT) profiles. The results were used to document the deformation pattern of rocks with the Miocene and the Holocene (400 ka travertine) in ages. By means of the investigations, deformation patterns implying the tectonic regimes during the Oligocene–Miocene–Pliocene, and Quaternary time have been determined. According to detailed field work, the local principal stress direction has been defined as approximately N35°W. This is also supported by the joint set and slip-plane data. Moreover, Oligocene–Miocene units provide a similar principal stress direction. Our data suggest that the southern part of the Elmalık fault is characteristic of reverse faults rather than of the normal fault system that has been previously reported. In addition, the Gürpınar fault controlling the deformation patterns of the region is a reverse fault with dextral component.

Keywords: deformation pattern, travertine, Van–Edremit area, Eastern Turkey.

Introduction

The Arabian (from south to north) and Eurasian (from north to south) plates move towards each other at a relative rate of 15–20 mm/yr. Eastern Anatolia has been squeezed between these two mega-plates and enormous tectonic activity has been manifested (Şengör & Yılmaz 1981; Şengör et al. 1985; Dewey et al. 1986; Koçyiğit et al. 2001; Oruç et al. 2017). This tectonic activity has caused the formation of a number of faults, complex structures and a very strange plateau, which have been reported by many scientists (Ketin 1977; Aksoy & Tatar 1990; Koçyiğit et al. 2001; Örçen et al. 2004; Dhont & Chorowicz 2006; Şengör et al. 2008; Üner et al. 2010; Koçyiğit 2013). The studies have some controversial results related to fault types, current tectonic regime, and deformation patterns. In addition, the most recent events of 23rd October, 2011 Van earthquake (Mw=7.1) and 9th November, 2011 (Mw=5.7) earthquakes by having its epicentres located on Edremit (Van) district have encouraged these discussions. After the earthquakes, some national and international researchers have been attracted to the area to investigate different characteristics of the places and recent earthquakes (Özkaymak et al. 2011; Koçyiğit 2013).

The faults giving rise to the 2011 main shock were not known until the two main earthquakes and were not indicated

on the active fault map of Turkey by Şaroğlu et al. (1992). On the other hand, Ambraseys & Finkel (1995) reported that many disastrous earthquakes around the Province of Van are known from historical records. One of them was the 1646 earthquake that caused significant loss in the Hoşap–Van region. A huge number of medium to small-sized earthquakes have also been recorded in and around Van city in the instrumental time.

The existences of active faults and their effect on the Oligocene–Quaternary units are the main target in recent study. Some of them have been reactivated and led to the occurrence of devastating earthquakes. The study of these faults and deformations of units in different ages could indicate the types of tectonic regimes and deformation in the aforesaid units.

In the content of this paper, two main subjects have been investigated: (1) geological and geophysical field data to describe the types of active faults that are the source of strong earthquakes, because there is a controversial issue about the types of fault in the study area, and (2) to study the deformation style of the Late Quaternary aged travertine to define the deformation style during the neotectonic period and the comparison of the results with Oligocene–Miocene units. It is the only way to understand the older and younger deformation patterns around Van city.

Geological settings

Tectonic significance

The Van region and its surroundings are located on the northern side of the Bitlis–Zagros Suture Zone (BZSZ) in the East Anatolian–Iranian Plateau, which has been formed from the collision between the Eurasian and Arabian Plates in the Late Miocene (Şengör & Kidd 1979; Şengör & Yılmaz 1981). The Anatolian Plate has two mega shear fault systems with dissimilar sense of motion in lateral direction, dextral North Anatolian Fault (NAF) and sinistral East Anatolian Fault (EAF). These two structures join with each other around Karlıova Triple Junction (KTJ) in Eastern Anatolia (Fig. 1).

Different ideas have been proposed about their initiation ages and the initiation of the neotectonic period. The movement of the Arabian Plate towards the Eurasian Plate occurring along the BZSZ has been continuing from the Serravalien (~12 Ma) to the present (Şengör & Yılmaz 1981). On the other hand, the initiation age of a strike-slip faulting-dominated neotectonic regime is proposed as Pliocene represented by N–S compressional axis (σ_1) (Koçyiğit et al. 2001; Dhont & Chorowicz 2006; Gürboğa 2015). Not only the initiation of the neotectonic period in Eastern Anatolia, but also the types of faults have been discussed in literature. Göğüş & Pysklywec (2008) claim that the lithospheric thinning is the main process in Eastern Anatolia that results in plateau uplift, heating, and syn-convergent extension resulted from the delamination of

the mantle lithosphere and the sites of contraction are only in the northern and southern margins. The Kağızman, Tuzluca, Hınıs, Karlıova, and Muş are located in extensional basins that have been controlled by E–W trending normal faults. Thus, the extension has been reported as the syn-convergent extension (Göğüş & Pysklywec 2008). In contrast, the nature of both geological features and their deformation style detected in the East Anatolian Plateau are related to strike-slip motions triggered by transpressional regime (Koçyiğit et al. 2001; Dhont & Chorowicz 2006). For example, sinistral strike-slip fault zones are named as the Horasan, Digor, Kağızman, Başkale, Posof; dextral strike-slip fault zones as the Pambak–Sevan, Salmas, Çaldıran, Erciş and the Yüksekova, and the Muş–Gevaş thrust to reverse fault zones (Arpat et al. 1977; Koçyiğit et al. 2001; Şaroğlu & Yılmaz 1986; Şaroğlu et al. 1987; Cisternas et al. 1989; Rebai et al. 1993; Dhont & Chorowicz 2006; Horasan & Boztepe-Güney 2007). Global positioning system (GPS) has indicated 18 ± 2 mm/year in the N24°W direction for the Arabian Plate in the south of BZSZ and that this north-westward motion of the Arabian Plate is mostly transmitted to Eastern Anatolia (McClusky et al. 2000; Reilinger et al. 2006; Utkucu 2013).

Seismicity of the region

The Lake Van Basin and its surroundings have a number of faults that play important roles in the deformation of the area and the occurrence of earthquakes (Ambraseys & Finkel 1995;

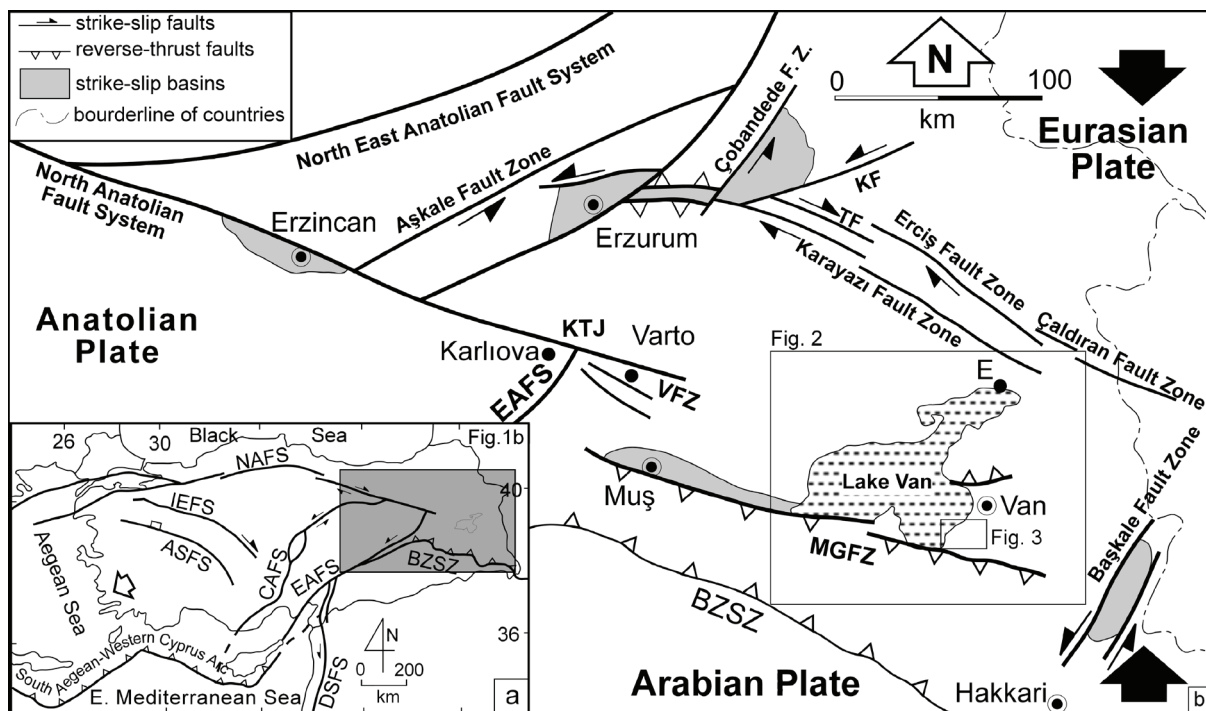


Fig. 1. a — Location map of Eastern Turkey. ASFS: Akşehir-Simav Fault System, BZSZ: Bitlis-Zagros Suture Zone, CAFS: Central Anatolian Fault System, EAFS: East Anatolian Fault System, IEFs: İnönü-Eskişehir Fault System, NAFS: North Anatolian Fault System; b — simplified tectonic map of East Anatolian–Iranian Plateau and adjacent areas (modified from Koçyiğit 2013) and E: Erciş, KF: Kağızman fault zone, MGFZ: Muş–Gevaş thrust to reverse fault zone, TF: Tutak fault, VFZ: Varto fault zone. Locations of Figs. 1b, 2 and 3 are inserted on the map.

Guidoboni et al. 1994). From the historical and instrumental records, earthquakes with various magnitudes have been recorded.

Historical earthquakes

The intensity of historical earthquakes has a range between I=V to X (Fig. 2, Table 1). Some of these earthquakes caused damage and loss of lives (Ambraseys & Finkel 1995). The records indicate earthquakes and their destructive results in the years 1101, 1646, 1715, and 1881 A.D. although there is no information about the earthquake source. For example, the 1646 earthquake has a I=X value, but the location of its epicentre is not clear. The areas near Gevaş and Gürpınar in the west and Hoşap through east and all rural areas that remain at its west along E–W trending were affected (Ambraseys & Finkel 1995) (Fig. 2). It is strongly probable that the Gürpınar Thrust Fault is the source of this event. No damage was reported on the southern side of the fault (foot-wall block). Another example is the A.D. 1101 earthquake. It caused

damage in Van city and its surrounding areas and formed wide fractures on the surface (Erdem & Lahn 2001). The source fault of this earthquake is also uncertain and this can be associated with the thrust faults cited in literature (Erdem & Lahn 2001).

Instrumental earthquakes

The most recent earthquake that caused the damage and loss of life around Van was the Tabanlı (Van) earthquake of 23rd October, 2011. Another one sourced from the Çaldıran Fault is the Çaldıran earthquake that took place in 1976 with the magnitude of M=7.3. The earthquake resulted from a dextral strike-slip fault and 380 cm displacement at the surface has happened (Arpat et al. 1977). After the earthquake, shaking activity continued in the area in 1976 and 1977 and many of the faults were reactivated. However, the magnitudes of the aftershocks remained around M=5.5. The Çaldıran earthquake did not affect Van city and nearby villages much and it mostly caused damage in the northern sections.

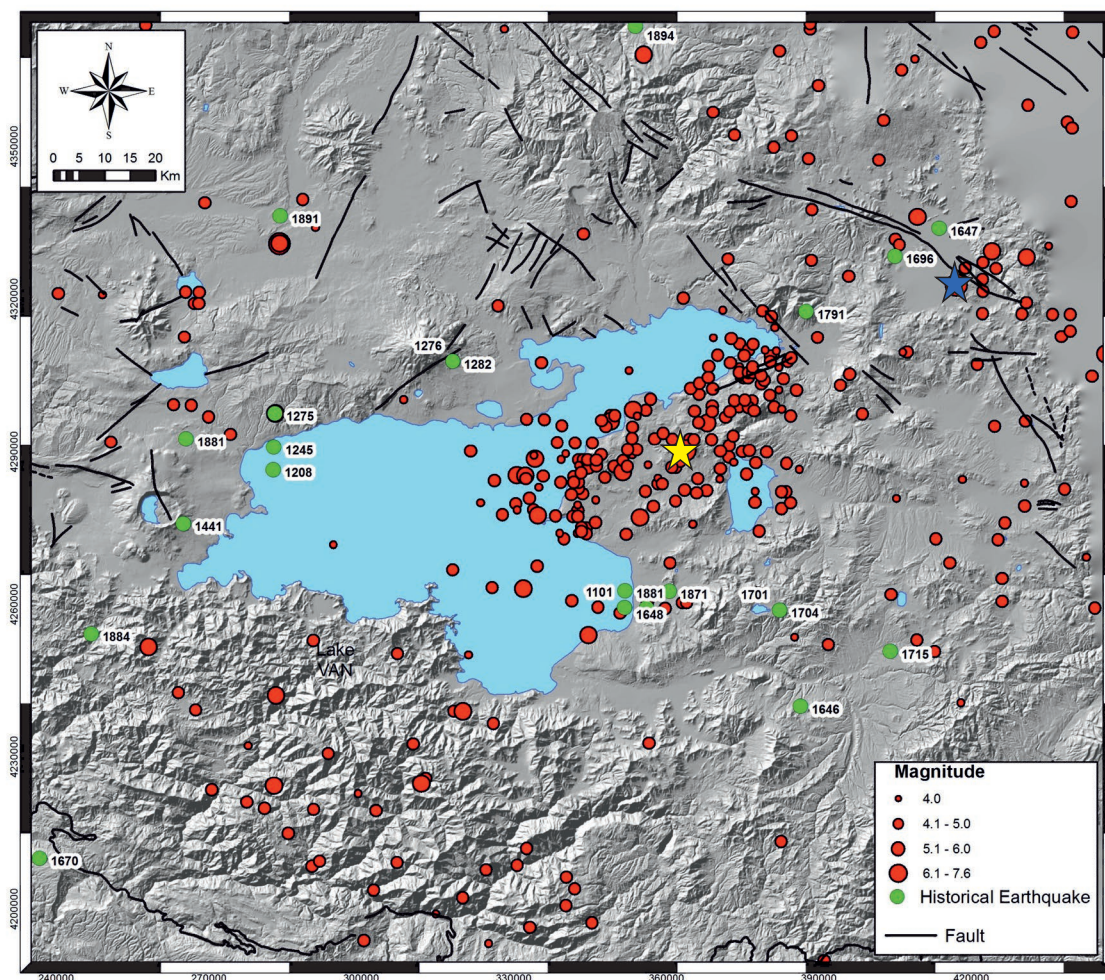


Fig. 2. Epicentres of historical (green points) and instrumental (red points) period earthquakes around Lake Van (earthquakes from KOERI 2009, 2011 and active faults from Emre et al. 2013). Yellow and blue stars indicate the epicentral location of the 23rd October, 2011 Van earthquake and Çaldıran earthquake, respectively.

Table 1: List of historical earthquakes which occurred around the Lake Van Basin (KOERI: Kandilli Observatory and Earthquake Research Institute 2009, 2011).

Latitude	Longitude	Date	M	I	Location	Reference
40	44	869	6.5	IX	Erivan	KOERI
38.47	43.3	1101	5	VI	Van	Ergin et al. 1967
38.47	43.35	1111	6.6	IX	Van	Erdem & Lahn 2001; Ergin et al. 1967; Soysal et al. 1981; Tan et al. 2008
38.7	42.5	1208	6.5	?	Ahlat–Van–Bitlis	Tan et al. 2008
38.74	42.5	1245	5	VII	Ahlat–Van–Bitlis–Muş	Ergin et al. 1967; Soysal et al. 1981; Tan et al. 2008
38.8	42.5	1275	6.8	?	Ahlat–Van	Tan et al. 2008
38.9	42.9	1276	5	VII	Ahlat–Erciş–Van	Ergin et al. 1967; Soysal et al. 1981; Tan et al. 2008
38.9	42.9	1282	5	?	Ahlat–Erciş	Soysal et al. 1981; Tan et al. 2008
38.6	42.3	1439	5	VI	Van–Bitlis–Muş	Ergin et al. 1967; Soysal et al. 1981; Tan et al. 2008
38.35	42.1	1441	5	VIII	Van–Bitlis–Muş	Ergin et al. 1967; Soysal et al. 1981; Tan et al. 2008
38.3	43.7	1646	6.7	X	Van	Ambraseys & Finkel 2006; Tan et al. 2008
39.15	44	1647	6.5	IX	Van–Tebriz–Bitlis–Muş	Soysal et al. 1981; Tan et al. 2008
38.47	43.3	1648	6.8	VIII	Hoşap–Van	Soysal et al. 1981; Ambraseys & Finkel 2006; Tan et al. 2008
39.1	43.9	1696	6.8	IX	Van	Tan et al. 2008
38.47	43.65	1701	5	VII	Van	Ergin et al. 1967; Soysal et al. 1981; Ambraseys & Finkel 2006; Tan et al. 2008
38.47	43.65	1704	5	VII	Van	Ergin et al. 1967; Soysal et al. 1981; Ambraseys & Finkel 2006; Tan et al. 2008
38.4	43.9	1715	6.6	VII	Van–Erciş	Ergin et al. 1967; Soysal et al. 1981; Ambraseys & Finkel 2006; Tan et al. 2008
39	43.7	1791	5	VI	Van–Tebriz–Erzurum	Ergin et al. 1967
38.5	43.4	1871	6.9	VII	Van	Ergin et al. 1967; Soysal et al. 1981; Tan et al. 2008
38.75	42.3	1881	7.3	IX	Van–Bitlis–Nemrut	Soysal et al. 1981; Ambraseys & Finkel 2006; Tan et al. 2008
38.5	43.3	1881	5	VII	Van and Nemrut region	Ergin et al. 1967
38.4	42.1	1884	6.1	V	Van	Ergin et al. 1967; Soysal et al. 1981

The earthquakes that affected Van city and the study area are $M=5.4$ in 1988, $M=5.3$ in 2000, and $M=4.7$ in 2001. These earthquakes did not cause any destruction around the Lake Van area (Fig. 2). The focal mechanism solutions of the events indicate that they are related to reverse faulting with strike-slip component (KOERI 2009).

To understand the structures that gave rise to the earthquake, the distribution of aftershocks belonging to the Tabanlı earthquake should be examined. The epicentre of this earthquake has been given as around the Edremit district and the general trend is N–S direction. Moreover, left lateral strike-slip movement is the characteristic feature (Koçyiğit 2013). On the other hand, both the earthquake distributions and the acceleration values indicate that the earthquake resonance was closer to E–W directions than N–S directions (Poyraz et al. 2011; Şengül et al. 2012). Except for this earthquake, no earthquake with a magnitude of more than $M=4$ has happened in the research area and its surroundings. According to our field work, we defined and mapped some main faults. When the trace of faults could not be seen at the surface, ERT profiles were used to understand the structure beneath the surface.

Stratigraphic outline

There is diversity in types and ages of rock units around the Lake Van region ranging from Paleozoic to Holocene. The region consists of metamorphic rocks of the Bitlis Massif in the south, Upper Cretaceous ophiolites in the east, and Cenozoic marine sediment on the southern shore of Lake Van. Detailed unit description is not the scope of the current study, but a short description has been given below. The formations

that outcrop in the southern part of Lake Van are the Bitlis Massif, Yüksekova Complex, Lake Van Formation, Edremit Travertine, and recent sediments (Aksoy 1991; MTA 2007; Koçyiğit 2013). The Lake Van Basin is underlain by Upper Paleozoic rocks in the south, the Campanian–Maastrichtian Yüksekova Complex in the north-east, the Oligocene–Miocene Van Formation consisting of conglomerate, sandstone, claystone, and limestone intercalation with turbidites, the Pliocene Kurtdeği Formation composed of red conglomerate, sandstone, claystone alternation in the east, and Quaternary travertine, fluvial–lacustrine clastic rocks in the east of Lake Van (MTA 2007; Acarlar et al. 1991). The Late Paleozoic basement consists of marble, recrystallized limestone, amphibolite, quartz–amphibole schist, and actinolite schist. The Yüksekova Complex consists of a mixture of various calc–alkaline volcanites, deep sea pelagic limestone to radiolarite–radiolarian chert, mudstone, greywacke, and all-sized tectonic slices of pillow lava, diabase, gabbro, and serpentinized peridotite derived from both the oceanic crust and uppermost mantle (Perinçek 1978). The formations that outcrop in the study area are the Van Formation, Kurtdeği Formation, Edremit Travertine, and the Lake Van Formation (Fig. 3). The Van Formation tectonically overlies the Plio–Quaternary colluvium units. It consists of sandstone, marl, claystone, and conglomerate.

The target rock unit, which has been observed on the southern side of Edremit settlement is the Edremit Travertine. The formation is located between the Oligocene–Miocene Van Formation and Quaternary Lake Van Formation in the study area and is bordered by the Gürpınar and Elmalık thrust faults (Fig. 3). The deformation patterns of the area during the neotectonic period can be observed in the Edremit Travertine, which has

been dated to 400 ka years (Degens et al. 1978). The travertine deposit is 50–70 m thick and is observed mostly between Edremit and Gevaş settlements (Fig. 3). It was first studied by Valeton (1978) and then mapped and named by Acarlar et al. (1991) as the Edremit Travertine that is extremely fissured, brecciated, and faulted (Örçen et al. 2004). Characteristics of the current and active deformation in the travertine were revealed by the position of the layer and joint systems. In the scope of this, bedding and joint measurements have been realized within the study area and the active stress state have been determined.

Methodology

In the scope of this study, geological mapping, fault-slip data, and identification of sub-surface structures by Electrical Resistivity Tomography (ERT) study have been applied. To be more specific, these methods meant: (a) geological mapping to identify the spread of units and their stratigraphic associations; (b) deformation forms of faults and units to clarify the types of tectonic regimes; (c) measurements from beddings, joints (the program “DIPS” was used), faults’ slip data (the program “Win-Tensor” was used) to reveal the dominant stress distribution on the area and their differences; (d) to evaluate and recognize the types of faulting; (e) ERT images have been used to see the continuation of the faults under the surface.

The first two methods have been applied during the fieldwork and geological mapping. The third and fourth ones are numerical approaches for the kinematics of the structures. By using the measurements from beddings and joints sets, their dominant directions and rose diagrams have been determined

with the program “DIPS”. Thus, fault-slip data were analyzed by using the Win-Tensor program with P–T–B method to determine the size and orientation of the principle stress directions. In this program, principal stress directions have been defined for each fault separately and at least 3 measurements are required. During the field study, limited slip plane data could be found. Thus, the same measurements were used for one fault. In this case, only one plane was seen in the stress diagram.

The last method is the ERT method used to understand the sub-surface structures. It is used most widely on geophysical investigations that has been applied successfully in determining the fault zone under the surface (Demagnet et al. 2001; Caputo et al. 2003, 2007; Wise et al. 2003; Colella et al. 2004; Rizzo et al. 2004; Nguyen et al. 2005; Giocoli et al. 2008; Fazzito et al. 2009). The ERT method is one of the methods for verifying discontinuities under the surface. In our study area, six short cross-sections 2D ERT profiles have been conducted across and near the active faults. Geoelectrical data have been collected using a Super Sting R8/IP/SP with 84 electrodes instrument. Measurements of the apparent resistivity have been realized using the dipole–dipole (DD) and/or Wenner–Schlumberger (WS) configuration. Different electrode spacing was used for the resistivity measurements collected within the study area. Processing of the geoelectrical data pseudo section has been accomplished using the Earth Imager provided by the AGI Advanced Geosciences modelling software so as to achieve the 2D resistivity data inversion software. Some parts of major faults that could not be seen on the surface have been determined by the ERT images. It has been applied on the probable fault to verify its continuation under the surface. These methods provided new field data which led to precise findings about the controversial issues.

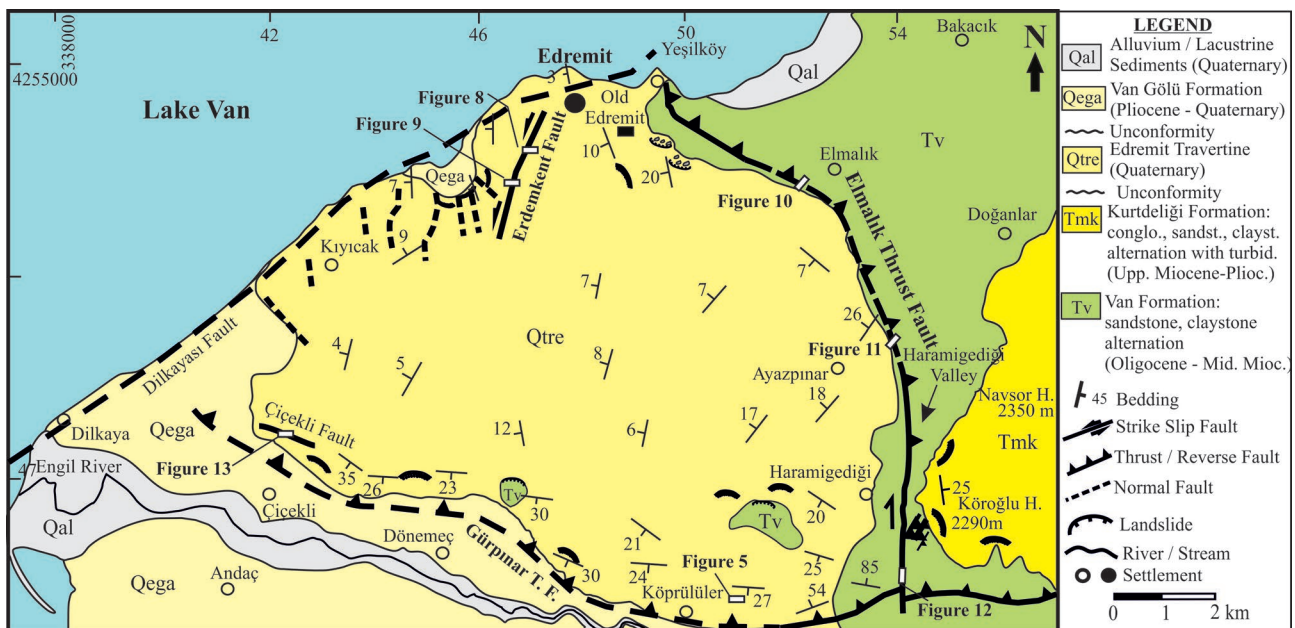


Fig. 3. Geological map of the study area indicating the Edremit Travertine and main features (modified from MTA 2007).

Interpretations

Structural analysis

Beddings

The travertine deposits predominantly strike in the NE–SW with their dip north-westward (Fig. 3). It seems that the bedding planes indicate a scattered pattern at the study area and main trend is determined by the WNW and the range of their dip angles are 5°–30° southward (Fig. 3). It is thought that the differences in the direction and dip angles have formed as a result of paleotopography during the formation of the travertine and/or as a result of the tilting linked with the compression. The E–W trending layers have been formed during the north-vergent thrusting. The SW dipping beds in the southern part of the area are related to the Gürpınar Thrust Fault and initial depositional conditions that indicate approximately NE–SW directed compressional axis. After the plotting, the dominant compression direction is NE–SW with NW-dipping (Fig. 4a).

Analysis of joints

The initial phases of buckling/bending of a layer resulted in open folds with a fixed wavelength/thickness proportion.

During this process, different trending joints could be formed in further stages depending on the thickness of bed, lithology and additional mechanisms (Bayly 1971, 1974; Bhattacharya 1992). Thus, some time-based distinctions in the distribution of joints and fissures during the folding (compression) depend on rheology for shallow crustal conditions. The development of fracture and joint patterns and distribution can radically change the rheology and mechanism of the forces (Ismat & Mitra 2005). In the mature periods of deformation, penetration of joints and fractures are the main components that control the deformation. From this result in the literature, it can be said that the different periods of deformation yield various joints and/or folding depending on the rheology. In many parts of our study area, joints that are crossing rigidly to each other have been observed (Fig. 5). The existence of joints with many different directions has been determined. The joints have dominantly been measured in the N10°E and N10°W trending. Moreover, two different trends in N75°E and N75°W have been measured. The first order set is in the approximately N10°W direction and repeating at average 100–300 cm distances. The second set is perpendicular to the first joint set in the NW-SE direction and with the wider distances compared with the first one. Even though a third joint set has been observed in the direction of NE–SW, field observation indicated that there is a high correlation between the third joint set and the second sets. Thus, these

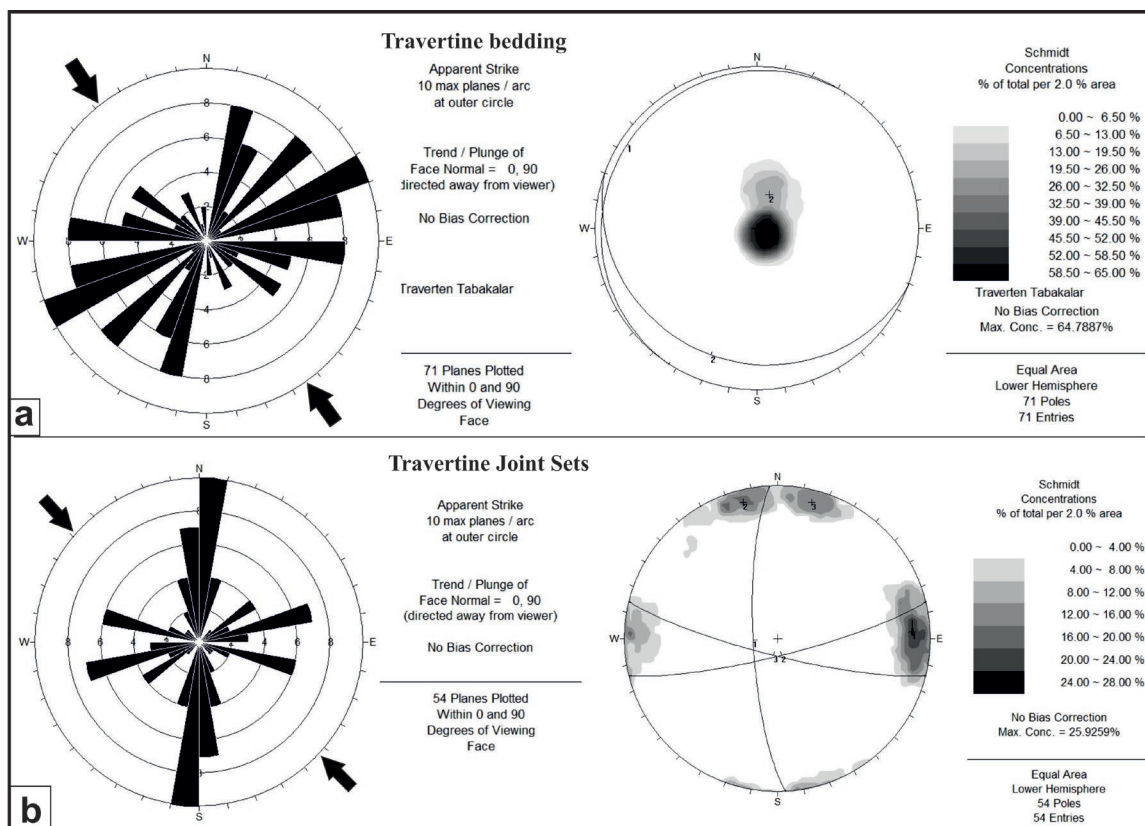


Fig. 4. Rose diagram and stereographic projection of bedding (a) and joint sets (b) in the Edremit Travertine. Approximate contraction force operating in the NW–SE direction. Fold axes have NE–SW-trends and a small amount of plunge. A rose diagram depicting the orientations of ground fractures measured in the field.

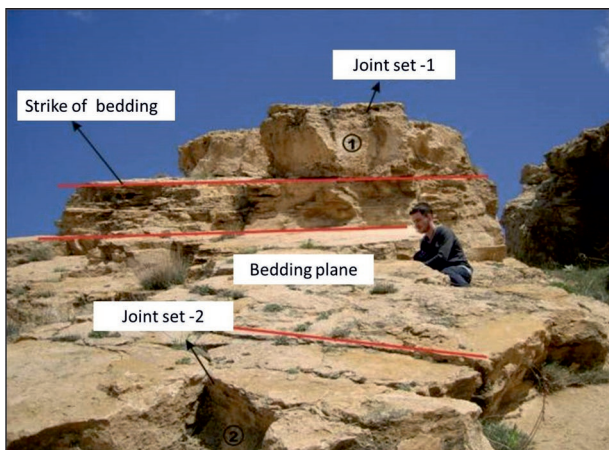


Fig. 5. Field photography of travertine showing two joint sets and bedding planes. Location of field photograph is given in Fig. 3.

planes have been evaluated together with the second set (Fig. 4b).

Fault-slip analysis

There are some active faults, which deform the Edremit Travertine that have been handled in detail in the scope of this study. Some of these faults have been mapped in the previous studies (Özkaymak 2003; Koçyiğit 2013). These faults have been observed in the northern and southern section of the Edremit Travertine as strike-slip and reverse faults, respectively. The existence and kinematics of these faults is important because of the young age (400 ka) of the Edremit Travertine. It gives chances to compare the active faults, which intersect the travertines and older faults, that occurred only in the Miocene deposits. If there is any difference between their characteristics, it can be evidence for tectonic regime differentiation. For example, the Oligocene–Miocene Van Formation is located under the travertine and it is deformed by reverse to thrust faults. The faulting within this area can be associated with the compression tectonic regime after the Miocene (Koçyiğit et al. 2001). These faults have the same character as the large scale reverse/thrust faults bordering the south and east of the study area (Fig. 6). The main faults that have been suggested in this research are named the Erdemkent, Elmalık, Gürpınar, and Çiçekli faults.

Together with the NE–SW trending beddings, the joints standing in ~E–W directions and slip-plane data from the fault surfaces, we detected the orientation of a compressional axis with an approximately NW–SE direction. Depending on the strike of fault, different types of faulting have been observed in the field. Slip plane measurements at diagrams 3, 4, 5, and 6 indicated dominantly reverse faulting with no or only minor strike slip component (Fig. 6). On the other hand, strike slip faulting with a minor amount of reverse component (diagram 1 in Fig. 6) and normal faulting with strike slip component (Fig. 6) in the releasing part of the faults could be observed in the study area.

ERT analysis

The morphological expressions of some faults could not be followed clearly on the surface. In those cases, geophysical methods are used to define the structures. In our study area, six ERT profiles were obtained with the order ERT-1 from the Erdemkent, ERT-2, 3, and 4 from Elmalık, ERT-5, and 6 from Gürpınar faults. The results of these profiles are given in Fig. 7. Subsurface resistivity views from related fault sections clearly indicate the location of discontinuities. ERT-1 shows that the Erdemkent fault is not interrupted as it is seen at the surface. Moreover, ERT-2 obtained in front of the Elmalık fault indicates the existence of some small scale faults.

Active faults

Erdemkent fault

The Erdemkent fault has been named in this study. Its name comes from the settlement just on the SE of the fault. The fault is clearly observed within the Edremit Travertine Unit (Fig. 8) and its dip direction is N80°W, 82°. This fault, that has been observed at the less resistant, shrub type travertine levels, is a left lateral strike slip fault with a minor normal component (Fig. 9). The displacement is about 30–40 cm at the travertine layers that have been observed through fault zone among the crashes and split offs (Fig. 8).

The southern half of the fault was mapped by Özkaymak (2003). During our field work, the northern continuation of the fault was observed and mapped. The southern part of the fault plane is measured in N110°E, 85°. It is uncovered in a stone quarry operated by Edremit Municipality. The slickenline was measured N30°E trending with a plunge of 64° SE (Table 2). A breccia zone about 5 m thick is observed in the fault zone (Fig. 9). Left lateral strike-slip faulting with a normal component has been analyzed from the slickenlines (Table 2).

Because of the slip data differences, the fault has two different motions, but the results of field observation suggest that they could be connected under the surface. Thus, determination of subsurface investigation by means of ERT survey has proved that these two faults are joined to each other that as the same with fault surface observation. The ERT-1 profile is placed to the north of the Edremit settlement (Fig. 6). 126 m long dipol–dipol (DD) array has been used, with 84 electrodes divided by 1.5 m. A maximum depth of 35 m has been modelled (Fig. 7a). The ERT-1 profile has been measured in the NW–SE direction that is perpendicular to the fault. The root mean square relative (RMS) error between the measurement and calculated apparent resistivity is small (3.55 %) implying that these interpretative results are good. The ascent has a small topographic relief and it is located at a distance of 36 m. The inverse model is consistent with the travertine unit. According to the figure, a weak strength travertine has been determined at about 10 m, suggesting that the low resistivity region in this part of the cross-section includes the space from

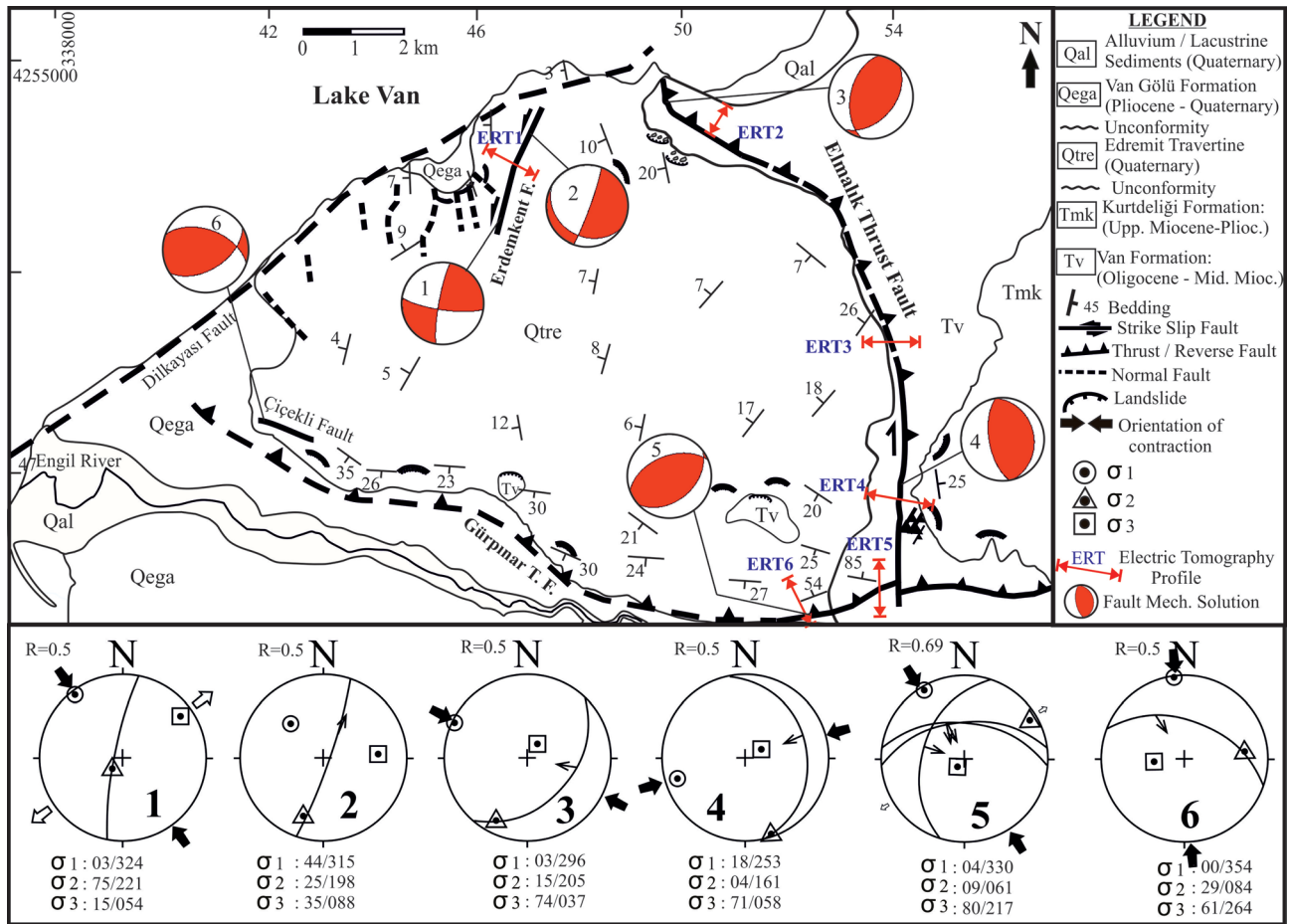


Fig. 6. Main tectonic features, bedding planes and ERT locations in the study area. Slip-plane data indicate the contractional regime dominantly.

place to place. Under this part of the cross-section, resistivity values are increasing with depth. The high resistivity amounts have been characterized by strong travertine because of the massive internal feature. Even, the slip data indicates different motion types; these two faults are actually a single fault. The reason for the differences is the various trend amounts of northern and southern parts of the faults connected with a buckling.

Elmalık Reverse fault

There are many discontinuity planes inside the Oligocene–Miocene aged Van Formation, which lie under the travertine formation. One of the most important structures is the Elmalık Reverse fault observed in the channel diggings with the strike and dip NW–SE and reverse character (Fig. 10) near Lake Van.

This fault starts in a N–S direction from the south side of the Haramigeđiği Valley, at its middle part after a bend it continues in a NW–SE trend up to the shore of Lake Van (Fig. 11a). This plane, dipping to the east, has developed inside the Oligocene–Miocene Van Formation. The Elmalık Reverse fault displaces the Gürpınar reverse fault in a dextral direction at the southernmost end and deforms younger sedimentary

strata at its northernmost side on the shore of Lake Van. Based on the field measurement, dip amounts are approximately 27° in the southern part and 70° in the northern part (Fig. 11b). According to our field measurements and ERT results, the Elmalık Reverse fault has two motions; dextral strike-slip and reverse on the southern and northern parts, respectively. Moreover, small scale reverse faulting has also developed in the sandstones belonging to the Van Formation to the south of the Haramigeđiği valley (Fig. 11c). With the effect of deformation formed after the Miocene, this type of reverse fault section with N120°E, 35° attitude is commonly observed (Şengül et al. 2012).

Three ERT surveys (ERT-2, ERT-3, and ERT-4 profiles seen in Fig. 6) have been obtained to determine the location of the Elmalık Reverse fault (Fig. 6). ERT-2 profile, which is a 252 m long DD array has been used along the profile with 84 electrodes separated by 3 m electrode spacing (Fig. 7b). Figure 7b shows the inverse model for the sub-surface resistivity results of the ERT-2 profile. The RMS error of the ERT-2 profile was 3.53 % after 2 iterations. The ERT-2 profile showing the low resistivity zone (5–25 Ωm) might be associated with a higher water content of the Oligocene–Miocene Van Formation. The ERT-2 profile shows between 72 and 105 m

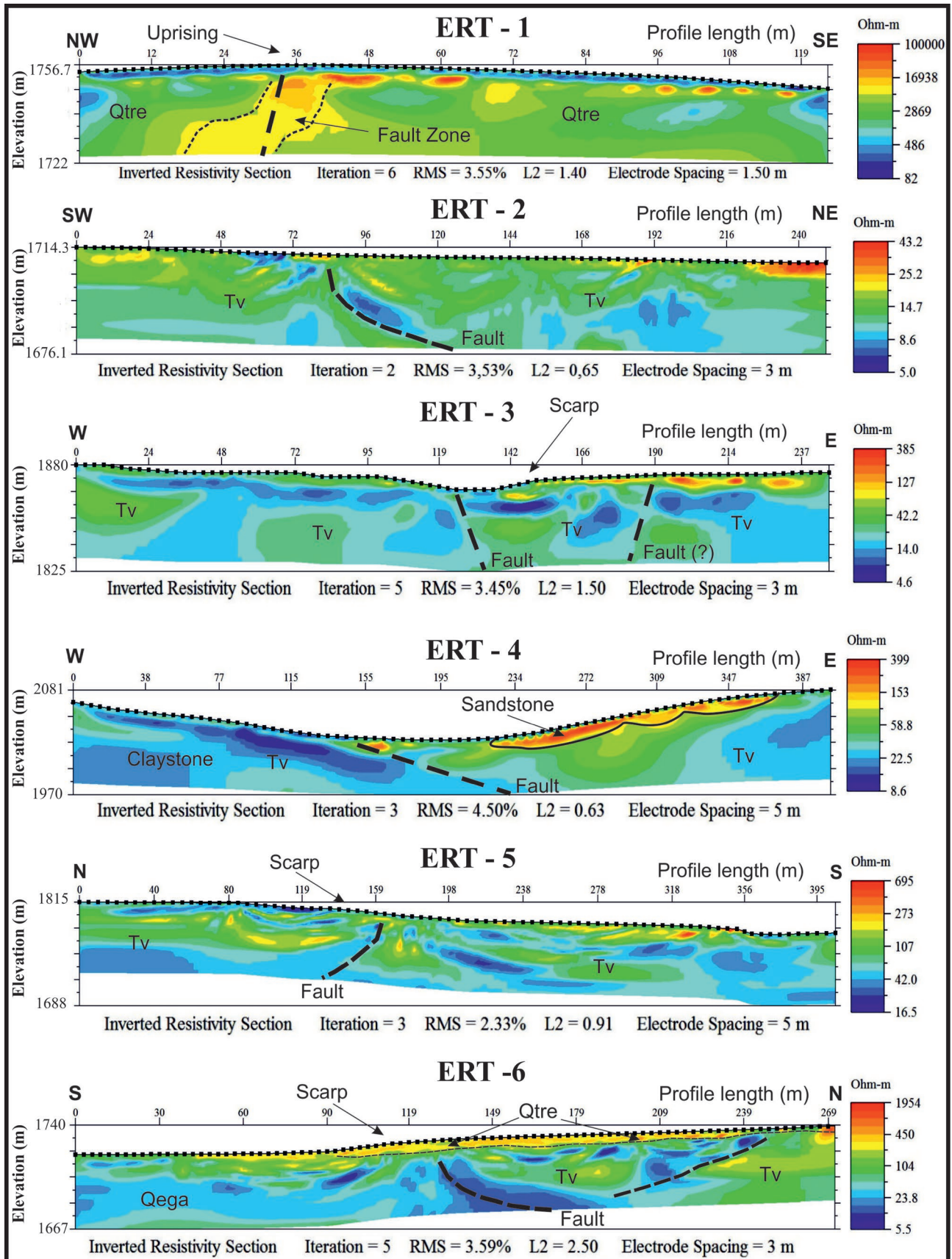


Fig. 7. ERT profiles show the apparent resistivity pseudosection inverse model for the subsurface resistivity results of the profiles ERT-1, ERT-2, ERT-3, ERT-4, ERT-5 and ERT-6 in the study area. Their locations can be seen at Fig. 6.

uplifted low resistivity unit from the S–W part of the cross-section. The N–S fault zone can be followed from the surface down to 35 m depth. In this section, reverse faulting has been seen within the Van formation and this has been interpreted as the Elmalık Reverse fault (Fig. 7b).

The ERT-3 profile has an E–W direction and a 252 m long DD array, with 84 electrodes separated by 3 m electrode

spacing (Fig. 7c). Figure 7c shows the inverse model for the subsurface resistivity results of the ERT-3 profile. The RMS error of the ERT-3 profile was 3.45 % after 5 iterations. The low resistivity zone (4.6–45 Ω m) shown by the ERT-3 profile can be related to the Oligocene–Miocene Van Formation. The eastern part of the cross-section includes high resistivity (127–385 Ω m), this part can be related to the Upper

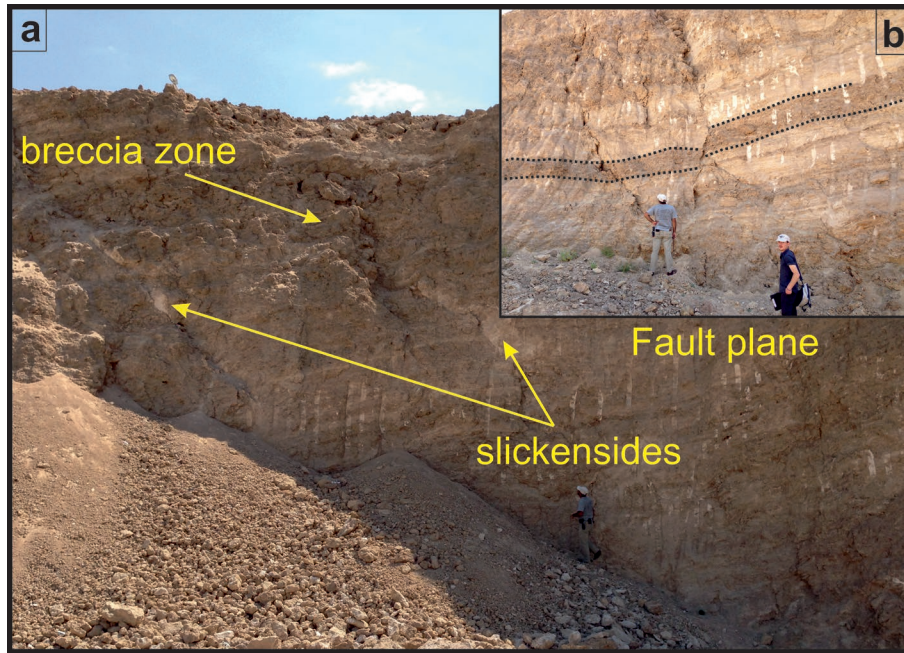


Fig. 8. General view of the Erdemkent fault plane (a), and 40 cm vertical displacement (b). Location of field photograph is given in Fig. 3.

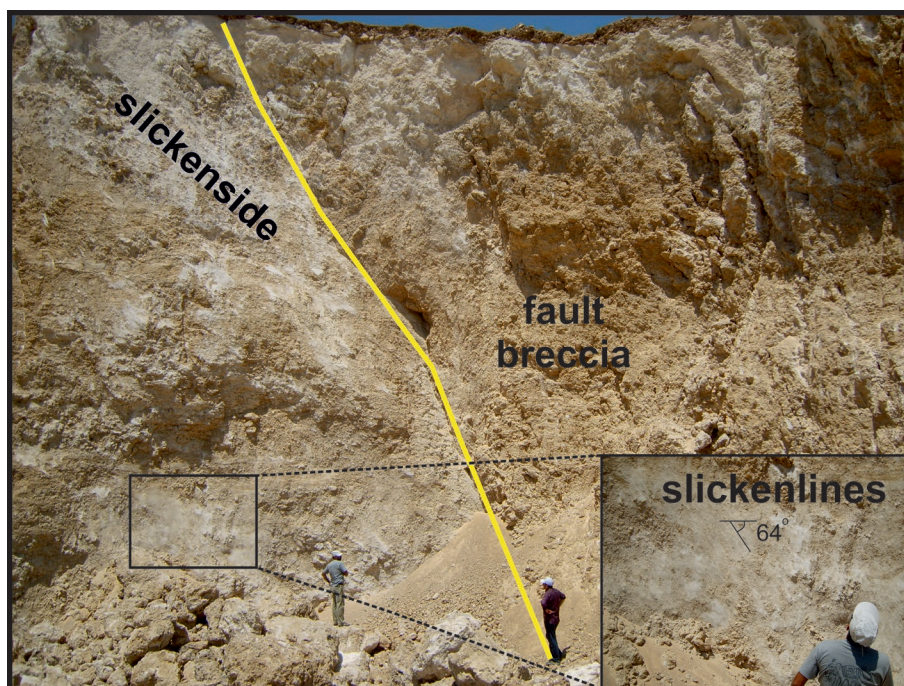









Fig. 9. General view of the Erdemkent fault plane, and breccia and slickenlines on the Erdemkent Fault. Location of the field photograph is given in Fig. 3.

Miocene–Pliocene Kurtdeliği Formation. The scarp has a small topographic relief and it is located at 148 m distance that shows and uplifted part on the eastern side. The ERT-3 profile has two faults. The first one is defined as the Elmalık Reverse fault between 119 and 142 m uplifted low resistivity unit from the N–S direction of the cross-section. The second fault is located at a distance of 190 m in the eastern part of the profile from the surface down to depth. The second fault is probably the antithetic fault of the Elmalık Reverse fault. ERT-4 profile is a 420 m long DD array, with 84 electrodes separated by 5 m electrode spacing (Fig. 7d). Figure 7d shows the inverse model for the subsurface resistivity results of the ERT-4 profile. The RMS error of the ERT-4 profile was 4.5 % after 3 iterations. The ERT-4 profile shows the low resistivity zone (8.6–40 Ω m) that could be related to the Oligocene–Miocene aged Van Formation. The eastern part of the cross-section includes high resistivity (153–399 Ω m), this part can be related to the Upper Miocene–Pliocene Kurtdeliği Formation. The ERT-4 profile shows a change between 145 and 195 m from low resistivity to high resistivity that defines the N–S Elmalık Reverse fault. The N–S fault can be followed from the surface down to 55 m depth.

Gürpınar Reverse fault

The Gürpınar Reverse fault has an E–W trend with a dip angle towards the north borderline between the travertine and the Lake Van Formation borderline in the southern section of the study

Table 2: Fault plane features and kinematic solutions (P–T axis) of faults in study area.

Fault	Plane's		Fault Line's		Fault Type	Kinematic Axes			Focal Mech.
	Dip Dir.	Dip	Trend	Plunge		σ_1	σ_2	σ_3	
1 Erdemkent	280	82	008	13	Sinistral/ Inverse	324/03	221/75	054/15	
2 Erdemkent	110	85	030	64	Normal/ Sinistral	315/44	198/25	088/35	
3 Elmalık	132	44	102	40	Inverse/ Dextral	296/03	205/15	037/74	
4 Elmalık	080	27	080	27	Inverse/ Reverse	253/18	161/04	058/71	
5 Gürpınar	354 290 005	55 50 55	330 285 335	57 57 50	Inverse/ Dextral	330/04	061/09	217/80	
6 Çiçekli	020	52	328	38	Inverse/ Dextral	354/00	084/29	264/61	
7 Tear Fault	084	84	355	08	Dextral/ Inverse	040/01	137/80	309/10	

area (Fig. 12). This fault is mostly observed within the Van Formation along a 12 km length in the study area and it extends 30 km more to the east up to the Engil valley (Kocyiğit 2013; Şengül et al. 2012). It is probably the last reverse fault on the southern side of the Eastern Anatolia Accretion Complex. It is thought that this fault is the source of the 1646 earthquake in the historical period (Ambraseys & Finkel 1995; Soysal et al. 1981). The deformation patterns are detected in the layers belonging to the Van Formation and the Travertine by reverse displacement. Measurements from the slickenline on the fault surface show that the fault is E–W trending with 50°–55° dip amount northwards, the slickenlines are NW–SE trending with 55° plunge amount (Table 2).

The electricity tomography method has been applied to the east section of the Gürpınar Reverse Fault (Fig. 6). ERT-5 profile is a 420 m length DD array, with 84 electrodes separated by 5 m electrode spacing (Fig. 7e). Figure 7e shows the inverse model for the subsurface resistivity results of the ERT-5 profile. The RMS error of the ERT-5 profile is 2.33 % after 3 iterations. The ERT-5 profile shows the low resistivity zone (10–45 Ω m) that can be related to the Oligocene–Miocene aged Van Formation. The cross-section includes partially high resistivity (>250 Ω m) values; these values can

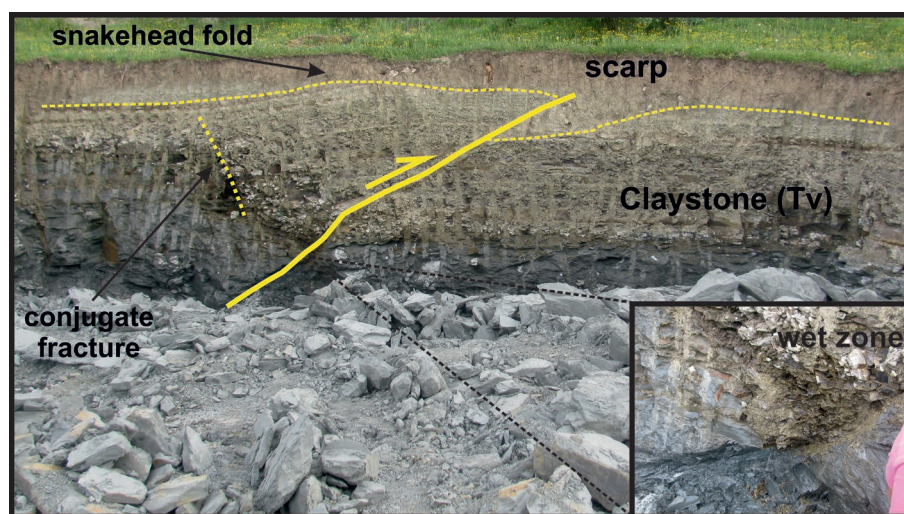


Fig. 10. General view of the Elmalık Reverse fault in an open pit, south of Edremit. Location of the field photograph is given in Fig. 3.

be related to the travertine slope rash blocks. The scarp has a minor topographic relief and it is located at a distance of 159 m, showing uplifted low resistivity units from the surface. The Gürpınar Reverse fault is seen in the inverse model for the sub-surface resistivity results. 159 m uplift is observed on the low resistivity unit relative to high resistivity unit along the E–W direction of the cross-section. The N part of the cross-section (at distance of 80 m) and S part of the section (at distance between 238 and 278 m) have been affected by the reverse faulting. The ERT-6 profile is located on N–S direction on the Gürpınar Reverse fault (Fig. 2). Figure 7f shows the inverse model for the subsurface resistivity results

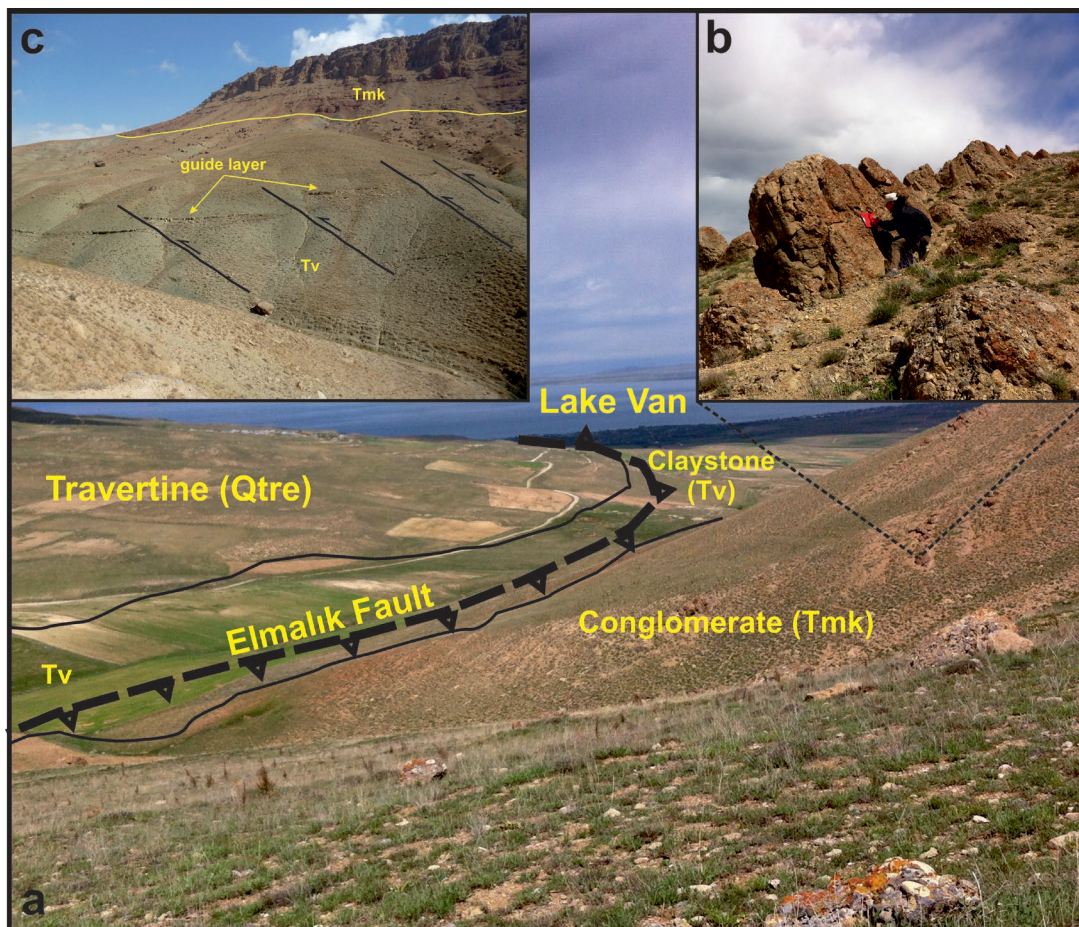


Fig. 11. General view of the Elmalık Fault on the northern part of Haramigediği Valley (a), steepened bedding of conglomerates in the Kurtdeliği Formation (b), small scaled reverse faults in the southern part of the Elmalık fault in Haramigediği Valley (c). Location of field photograph is given in Fig. 3.

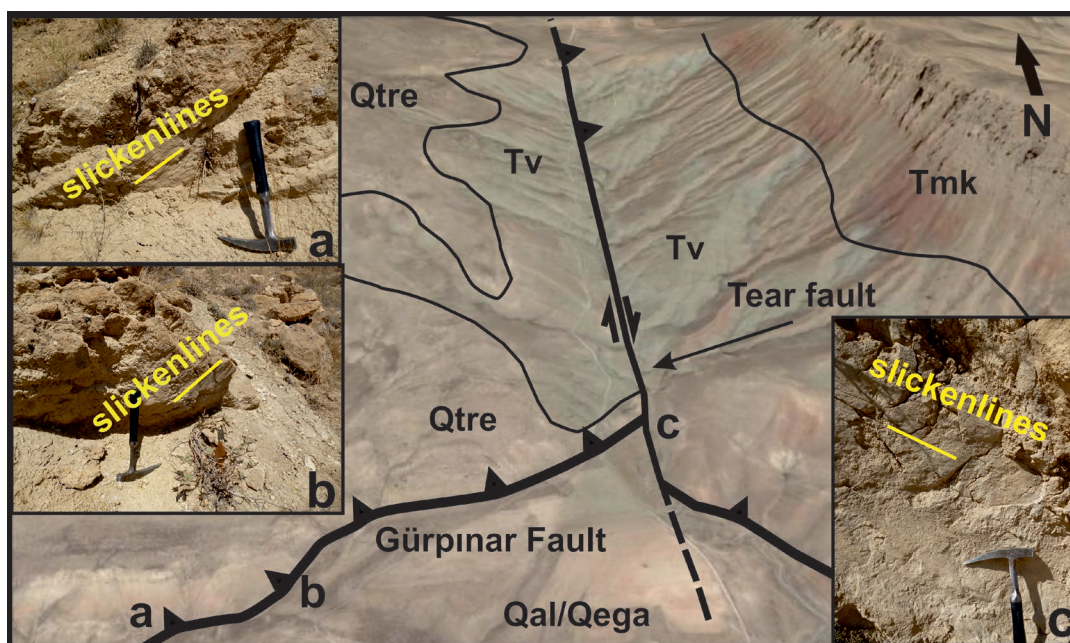


Fig. 12. Google Earth Image view of the Gürpınar Thrust Fault and its N-S trending tear fault, which is merged with the Elmalık fault in the Haramigediği Valley. Slickenlines of faults are shown in small pictures (a, b, c). Approximate location of field photograph is given in Fig. 3.

of the ERT-6 profile. The ERT-6 profile has a 272 m length with roll-along configuration DD array, with 84 electrodes separated by 3 m electrode spacing (Fig. 7f). The RMS error of the ERT-6 profile was 3.59 % after 5 iterations. Figure 7f indicates massive travertine about 10 m thick with high resistivity ($>450 \Omega\text{m}$) region in the cross-section. In the southern part of the cross-section, low resistivity values ($5\text{--}30 \Omega\text{m}$) can be related to an increased water content of the Quaternary aged Van Lake Formation. In the northern part of the cross-section, low-middle resistivity values ($30\text{--}120 \Omega\text{m}$) could be related to the Van Formation proving the uplift relative to the Van Lake Formation in the cross-section. The Gürpınar Reverse fault was determined along the E–W trend between 125 m and 140 m.

Çiçekli fault

The Çiçekli fault is placed on the south-east side of the Edremit Travertine and just at the north-east of Çiçekli Village (Fig. 6). The fault has a strike and dip of $N290^\circ\text{W}$, 52° and it nearly has the same trend as the Gürpınar Reverse Fault. The fault surface has been observed in a mine pit, but it is very difficult to follow its surface expression. The observable extent of the fault on the surface is about 1 km, where the travertine has been crushed and folded. Brown coloured fault clay is present along the crushed zone (Fig. 13). The slickenlines have NW–SE direction with a plunge of 38° to the NW (Table 2). Current colluvial materials have been deposited in front of the layers folded on top the fault. Because of the deformation in the travertine, the fault has been evaluated as active and it is conformable with the Gürpınar Reverse fault.

Discussion

According to previous geological and geophysical studies and all the data observed during our fieldwork, Eastern Anatolian has been experiencing $\sim\text{N-S}$ trending contraction that yields various structures such as reverse-thrust faults, strike-slip faults, oblique-slip normal faults, folds and different types of basins. The main shortening direction was determined from the bedding planes, kinematic analyses of joints and slickenlines of fault surfaces. Especially the slip plane data from the fault proved this result. The kinematic results of Gürpınar Reverse fault indicate that the dominant shortening direction is $N30^\circ\text{W}$. This fault emplaced the clastics derived from the Edremit Travertine and the Van Formation on top of the Plio-Quaternary unit located along the Engil Valley. This

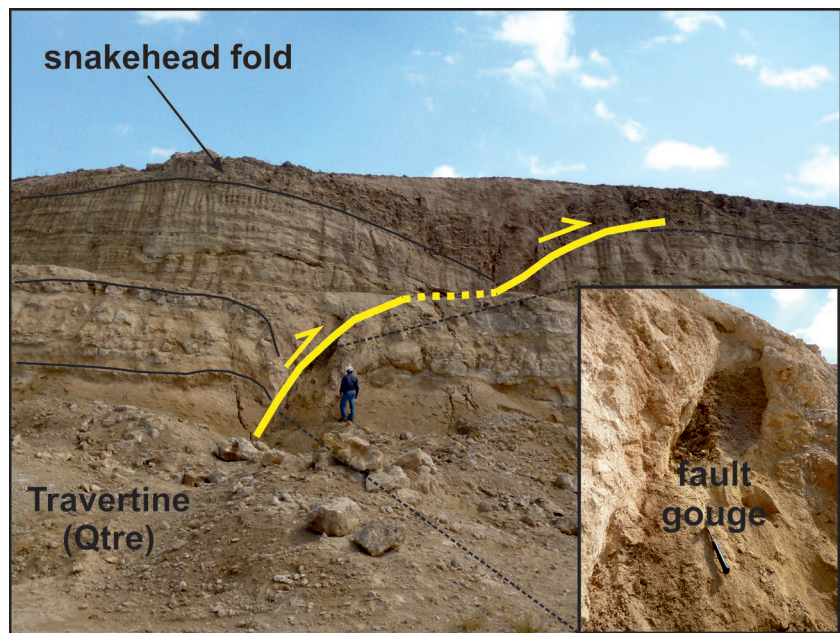


Fig. 13. General view of the Çiçekli Fault near Çiçekli village with dark brown fault gouge in the fault zone shown in the inset. Location of the field photograph is given in Fig. 3.

is the most important evidence for the reverse motion in that the younger unit is located under the older deposits. According to previous research, this fault produced the 1646 earthquake with the intensity of IX (Ambraseys & Finkel 1995). It probably indicates that the source of the 1646 earthquake is related to this thrust fault. Before the event, there is no historical record resulting from the fault. Approximately 350 years have already passed after the last event (1646) and it might be a seismic gap. The Gürpınar Reverse fault is ~ 40 km in length and in the case of accumulated stress, a destructive earthquake could be generated. From this perspective, the fault is very important for the area and it needs paleoseismological studies.

The Elmalık Reverse fault is another important structure in the study area. This fault was mapped by some authors, but with a different faulting character (Örçen et al. 2004; Özkaymak et al. 2004; Koçyiğit 2013). According to them, the Elmalık Reverse fault is a NW–SE trending thrust fault with right lateral component and interrupted by the Van Fault that is a N–S trending normal fault. This description defines the northern part of the Elmalık Reverse fault. On the other hand, the fault continues with a bending towards the south with small changes in type of fault. Thus, during our field work, thrust motion along the fault surface from slickensides and folds on the northern parts of Elmalık Reverse fault points out the compressional regime (Fig. 10). In the ERT results applied under the surface, thrust motion of the same units were detected along the southern half of the fault (ERT-2, ERT-3, and ERT-4). At the southern end of the Elmalık Reverse fault, strike-slip motion with thrust component has been observed and measured (Fig. 12). Thus, dextral displacement along

the Elmalık Reverse fault cut and displaced the Gürpınar Thrust fault (Fig. 12).

In this study, a number of small scale faults have been observed and measured deforming the Plio-Quaternary Edremit travertine. According to their single plane solutions, approximately N35°W compression direction has been determined.

Conclusions

Based on this study, we can conclude that:

- Totally, 71 measurements have been collected from bedding planes showing mostly NE–SW trending, north-western dipping in the northern and ENE–WSW-trending, north-western dipping planes in the southern side of the area.
- The Edremit Travertine is an important deposit in that it records the recent deformation history in the area. The results indicate that the main compression direction is approximately N35°W (Fig. 6). The travertine records two different motions on the faults. It means that the geological evolutionary history of the area included at least two different tectonic regimes.
- The upper layers of the travertine deposit to be in the soft-porous rock quality as lithological have made it difficult to observe the joint sets clearly over a large area (Ismat & Mitra 2005). This fact has caused the developing joints to be widely separated and have gaps. 54 measured joint planes belonging to the travertine have a N–S trend that is conformable with the direction of left lateral strike-slip faults deforming the travertines. Mainly, three groups of joint sets have been defined in the travertine (Fig. 4b)
- The contraction direction N35°W has been proved by the joints and beddings developed in the Edremit Travertine. It supports recent configurations of principal stress axes.
- The Elmalık reverse fault has a bend at its middle sector and these two parts (northern and southern). This bending creates a different character in faulting. The northern part is a reverse fault with dextral component and southern part is a dextral strike-slip fault with reverse component.
- The Elmalık Reverse fault is a tear fault in its southern edge that deforms the Gürpınar Reverse fault in dextral displacement.

Acknowledgements: This article includes some results of doctoral research which was supported by Istanbul University Research Fund (project no:19486) of first author. The authors would like to thank Prof. Hayrettin Koral for editing and guiding this paper. Our students from Van Yuzuncu Yil University Department of Geology were helpful on field studies, we would thank their effort too. The authors are also grateful for support of Handling Editor Prof. Rastislav Vojtko spending much time for editing this paper. Finally, the reviewers are appreciated. Their suggestions and critical reading significantly improved this manuscript.

References

- Acarlar M., Bilgin Z.A., Erkal T., Güner E., Şen A.M., Umut M., Elibol E., Gedik İ., Hakyemez Y. & Uğuz M.F. 1991: Geology of East and North of Lake Van [Van Gölü Doğu ve Kuzeyinin Jeolojisi]. *Open file report, Mineral Research and Exploration Archive*, No: 9469, 1–93 (in Turkish).
- Aksoy E. 1991: Stratigraphy of the east-northeastern region of Van city [Van şehri doğu-kuzeydoğu yöresinin stratigrafisi]. In: *Geology Symposium of Ahmet Acar. Çukurova University, Adana*, 1–10 (in Turkish).
- Aksoy E. & Tatar Y. 1990: Stratigraphy and tectonics of the east-northeastern region of Van city [Van İli doğu-kuzeydoğu yöresinin stratigrafisi ve tektoniği]. *TUBITAK Journal of Nature* 14, 628–644 (in Turkish with English abstract).
- Ambraseys N.N. & Finkel C.F. 1995: The seismicity of Turkey and adjacent Areas: A historical review 1500–1800. *Eren publishing and booktrade*, İstanbul, 1–240.
- Arpat E., Şaroğlu F. & İz H.B. 1977: 1976 Çaldıran earthquake. *Earth and Human* 2, 1, 29–41.
- Bhattacharya A.R. 1992: A quantitative study of hinge thickness of natural folds: some implications for fold development. *Tectonophysics* 212, 371–377.
- Bayly M.B. 1971: Similar folds, buckling and great circle patterns. *J. Geol.* 79, 110–118.
- Bayly M.B. 1974: An energy calculation regarding the roundness of folds. *Tectonophysics* 24, 291–316.
- Caputo R., Pitsitelli S., Oliveto A., Rizzo E. & Lapenna V. 2003: The use of electrical resistivity tomographies in active tectonics: examples from the Tynavos Basin, Greece. *J. Geodyn.* 36, 19–35.
- Caputo R., Salviulo L., Pitsitelli S. & Loperte A. 2007: Late Quaternary activity along the Scorcibuoi Fault (Southern Italy) as inferred from electrical resistivity tomographies. *Annals of Geophysics* 50, 2, 213–224.
- Cisternas A., Philip H., Bousquet J.C., Cara M., Deschamps A., Dorbath L., Dorbath C., Haessler H., Jimenez E., Nercessian A., Rivera L., Romanowicz B., Gvishiani A., Shebalin N.V., Aptekman I., Arefiev S., Borisov B.A., Gorshkov A., Graizer V., Lander A., Pletnev K., Rogozhin A.I. & Tatevissian R. 1989: The Spitak (Armenia) earthquake of 7 December: field observations, seismology and tectonics. *Nature* 339, 675–679.
- Colella A., Lapenna V. & Rizzo E. 2004: High-resolution imaging of the high agri valley basin (Southern Italy) with electrical resistivity tomography. *Tectonophysics* 386, 29–40.
- Degens E.T., Wong B.K., Kurtman F. & Finckh P. 1978: The Geology of Lake Van. *Open file report, Mineral Research and Exploration Archive*, No:169, 1–153.
- Demant D., Renardy F., Vanneste K., Jongmas D., Camelbeek T. & Meghraoui M. 2001: The use of geophysical prospecting for imaging active faults in the Roer Graben, Belgium. *Geophysics* 614, 1, 78–89.
- Dewey J.F., Hempton M.R., Kidd W.S.F., Şaroğlu F. & Şengör A.M.C. 1986: Shortening of continental lithosphere: the neotectonics of Eastern Anatolia — a young collision zone. In: Coward M.P. & Ries A.C. (Eds.): *Collision Tectonics. Geol. Soc. London Spec. Publ.* 19, 3–36.
- Dhont D. & Chorowicz J. 2006: Review of the neotectonics of the Eastern Turkish–Armanian Plateau by geomorphic analysis of digital elevation model imagery. *Int. J. Earth Sci. (Geol. Rundsch.)* 95, 34–49.
- Emre Ö., Duman T.Y., Özalp S., Elmacı H., Olgun Ş. & Şaroğlu F. 2013: Active Fault Map of Turkey, 1:1.125.000 [Türkiye'nin Aktif Fay Haritası, 1:1.125.000]. *General Directorate of Mineral Research and Exploration, Special Publication*, Ankara, Turkey, 30, 1–181. ISBN: 978-605- 5310-56-1 (in Turkish).

- Erdem N.P. & Lahn E. 2001: Earthquake Catalogue of Turkey with Explanation (Türkiye deprem Kataloğu). *Yıldız Technical University Publications*, No: IN-KT-2001.007, İstanbul, 1–63 (in Turkish).
- Ergin K., Güçlü U. & Uz Z. 1967: A catalog of earthquakes for Turkey and surroundings area [Türkiye ve Civarının Deprem Kataloğu] (MS. 11-1964). *ITU Publications* 28, 1–58 (in Turkish with English abstract).
- Fazzito S.Y., Rapalini A.E., Cortés J.M. & Terrizzano C.M. 2009: Characterization of Quaternary faults by electric resistivity tomography in the Andean Precordillera of Western Argentina. *Journal of South American Earth Sciences* 28, 217–228.
- Giocoli A., Magri C., Vannoli P., Piscitelli S., Rizzo E., Siniscalchi A., Burrato P., Basso C. & Di Nocera S. 2008: Electrical Resistivity Tomography investigations in the Ufita Valley (Southern Italy). *Annals of Geophysics* 51, 1, 213–223.
- Göğüş O.H. & Pysklywec R.N. 2008: Mantle lithosphere delamination driving plateau uplift and synconvergent extension in eastern Anatolia. *Geology* 36, 723–726.
- Guidoboni E., Compastri A. & Traina G. 1994: Catalogue of Ancient Earthquakes in the Mediterranean area up to the 10th century. *ING-SGA Book*, Vol. 1, Bologna, 1–504.
- Gürboğa Ş. 2015: Source fault of 19 August 1966 Varto earthquake and its' mechanism: New field data, Eastern Turkey. *Journal of Asian Earth Sciences* 111, 792–803.
- Horasan G. & Boztepe-Güney A. 2007: Observation and analysis of low frequency crustal earthquakes in Lake Van and its vicinity, Eastern Turkey. *J. Seismology* 11, 1, <https://doi.org/10.1007/s10950-006-9022-2>
- Ismat Z. & Mitra G. 2005: Folding by cataclastic flow: evolution of controlling factors during deformation. *J. Struct. Geol.* 27, 2181–2203.
- Ketin I. 1977: The main orogenic events and paleogeographic evolution of Turkey. *Bulletin of Mineral Research and Exploration* 88, 1–4.
- Koçyiğit A., Yılmaz A., Adamia S. & Kulashvili S. 2001: Neotectonics of East Anatolian Plateau (Turkey) and Lesser Caucasus: Implication for transition from thrusting to strike-slip faulting. *Geodin. Acta* 14, 177–195.
- Koçyiğit A. 2013: New field and seismic data about the intraplate strike-slip deformation in Van region, East Anatolian plateau, E. Turkey. *Journal of Asian Earth Sciences* 62, 586–605.
- KOERI 2009: A Catalogue of Source Parameters of Moderate and Strong Earthquakes for Turkey and its Surrounding Area (1938–2008) [Türkiye ve Çevresi Faylanma-Kaynak Parametreleri (MT) Kataloğu (1938-2008)]. *Boğaziçi University Publications*, No: 1026, 1–43 (in Turkish).
- KOERI 2011: Probabilistic Assessment of the Seismic Hazard for the Lake Van Basin, October. <http://www.koeri.boun.edu.tr> (last access: December 23, 2011).
- McClusky S., Balassanian S., Barka A., Demir C., Ergintav S., Georgiev I., Gürkan O., Hamburger M., Hurst K., Kahle H., Kastens K., Nadariya M., Ouzouni A., Paradissis D., Peter Y., Prilepin M., Reilinger R., Sanli I., Seeger H., Tealeb A., Toksöz M.N. & Veis G. 2000: GPS constraints on plate kinematics and dynamics in the Eastern Mediterranean and Caucasus. *J Geophys Res* 105, 5695–5719.
- MTA 2007: Geological Maps of Turkey. Van-K 50, Scale: 1:100,000; 1 sheet.
- Nguyen F., Garambois S., Jongmans D., Pirard E. & Loke M.H. 2005: Image processing of 2D resistivity data for imaging faults. *Journal of Applied Geophysics* 57, 260–277.
- Oruç B., Gomez-Ortiz D. & Petit C. 2017: Lithospheric flexural strength and effective elastic thicknesses of the Eastern Anatolian and surrounding region. *Journal of Asian Earth Sciences* 150, 1–13.
- Örçen S., Tolluoğlu A.Ü., Köse O., Yakupoğlu T., Çiftçi Y., Işık A., Selçuk L., Üner S., Özkaymak Ç., Akkaya İ., Özvan A., Sağlam A., Baykal M., Özdemir Y., Üner T., Karaoğlu Ö., Yeşilova Ç. & Oyan V. 2004: Investigation of Sedimentological Properties and Active Tectonism for Seismicity in Plio-Quaternary Sediments of Van City Urbanization Areas (Van Şehri Kentleşme Alanlarında Yüzeyleyen Pliyo-Kuvaterner Çökellerinde Sedimentolojik Özelliklerin ve Aktif Tektonizmanın Depremselliğe Yönelik İncelemesi). *TÜBİTAK-VAP Research Project YDABAG-101Y100*, 1–162 (in Turkish with English abstract).
- Özkaymak Ç. 2003: Active Tectonic Features of Van city and Surroundings. *MSc Thesis, Institution of Science, Van Yüzyüncü Yıl University*, 1–76.
- Özkaymak Ç., Yürür T. & Köse O. 2004: An example of intercontinental active collisional tectonics in the Eastern Mediterranean region (Van, Eastern Turkey). In: Fifth International Symposium on Eastern Mediterranean Geology (5th ISEMG). Thessaloniki, Greece, 153–156.
- Özkaymak Ç., Sözbilir H., Bozkurt E., Dirik K., Topal T., Alan H. & Çağlan D. 2011: 23 October 2011 Seismic Geomorphology of the Van Earthquake and its Relationship with Active Tectonic Structures in Eastern Anatolia [23 Ekim 2011 Tabanlı-Van Depreminin Sismik Jeomorfolojisi ve Doğu Anadolu'daki Aktif Tektonik Yapılarla Olan İlişkisi]. *Jeoloji Mühendisliği Dergisi — Journal of Geological Engineering* 35, 2, 175–200 (in Turkish with English abstract).
- Perinçek D. 1978: Southeast Anatolia autochthonous and allochthonous units geology symbols [Güneydoğu Anadolu otokton ve allokton birimler jeoloji sembolleri]. *TPAO Research Group*, No: 6657, 1–135 (in Turkish).
- Poyraz S.A., Şengül M.A. & Pınar A. 2011: 23 October 2011 Van-Tabanlı Earthquake Source Mechanism and Seismotectonic Interpretation [23 Ekim 2011 Van-Tabanlı Depremi Kaynak Mekanizması ve Sismotektonik Yorumu]. *İstanbul Yerbilimleri Dergisi — İstanbul Earth Sciences Journal* 24, 2, 129–139 (in Turkish with English abstract).
- Rebai S., Philip H., Dorbath L., Borisssoff B., Haessler H. & Cisternas A. 1993: Active tectonics in the Lesser Caucasus: coexistence of compressive and extensional structures. *Tectonics* 12, 1089–1114.
- Reilinger R., McClusky S., Vernant P., Lawrence S., Ergintav S., Cakmak R., Özener H., Kadirov F., Guliev I., Stepanyan R., Nadariya M., Hahubia G., Mahmoud S., Sakr K., ArRajehi A., Paradissis D., Al-Aydrus A., Prilepin M., Guseva T., Evren E., Dmitrova A., Filikov S.V., Gomez F., Al-Ghazzi R. & Karam G. 2006: GPS constraints on continental deformation in the Africa–Arabia–Eurasia continental collision zone and implications for the dynamics of plate interactions. *J. Geophys. Res.* 111, 3–36.
- Rizzo E., Colella A., Lapenna V. & Piscitelli S. 2004: High-resolution images of the fault-controlled High Agri Valley basin (Southern Italy) with deep and shallow electrical resistivity tomographies. *Phys. Chem. Earth* 29, 321–327.
- Soysal H., Sipahioğlu S., Kolçak D. & Altınok Y. 1981: Historical Earthquake Catalog of Turkey and its surroundings [Türkiye ve Çevresinin Tarihsel Deprem Kataloğu] (2100 B.C.–1900 A.D.). *TÜBİTAK Report TBAG-341*, 1–86 (in Turkish with English abstract).
- Şaroğlu F. & Yılmaz Y. 1986: Geological evolution and basin modeling in neotectonic period [Doğu Anadolu'da neotektonik dönemdeki jeolojik evrim ve havza modelleri]. *Bull. Miner. Res. Explor. Inst. (MTA)* 107, 73–94 (in Turkish).
- Şaroğlu F., Emre Ö. & Boray A. 1987: Active faults of Turkey and their seismicity [Türkiye'nin diri fayları ve depremsellikleri]. *Open file report, Mineral Research and Exploration Archive*, No: 8174, 1–14 (in Turkish).

- Şaroğlu F., Emre Ö. & Kuşçu İ. 1992: The East Anatolian fault zone of Turkey. *Ann. Tectonicae* VI, 99–125.
- Şengör A.M.C. & Kidd W.S.F. 1979: Post-collisional tectonics of the Turkish–Iranian plateau and a comparison with Tibet. *Tectonophysics* 55, 361–376.
- Şengör A.M.C. & Yılmaz Y. 1981: Tethyan evolution of Turkey: a plate tectonic approach. *Tectonophysics* 75, 181–241.
- Şengör A.M.C., Görür N. & Şaroğlu F. 1985: Strike-slip faulting and related basin formation in zones of tectonic escape: Turkey as a case study. In: Biddle K.T. & Christie-Blick N. (Eds.): Strike-slip Deformation, Basin Formation and Sedimentation. *Soc. Econ. Paleont. Mineral. Tulsa, Sp. Publ.* 37, 227–264.
- Şengör A.M.C., Özener S.M., Keskin M., Sakıncı M., Özbakır A.D. & Kayan İ. 2008: Eastern Turkish high plateau as a small Turkic-type orogen: Implications for post-collisional crust-forming processes in Turkic-type orogens. *Earth Sci. Rev.* 90, 1, 1–48.
- Şengül M.A., Koral H. & Altuncu S. 2012: 9 November 2011 Van Earthquake Possible Source Fault and Effects [9 Kasım 2011 Van Depremi Olası Kaynak Fayı ve Etkileri]. In: 16. Active Tectonics and Research Group Workshop, ATAG 16, İstanbul, 18–19 October 2012. *Abstract Book (Bildiri Özleri Kitabı)*, 38 (in Turkish).
- Tan O., Tapırdamaz M.C. & Yörük A. 2008: The Earthquakes Catalogues for Turkey. *Turkish Journal of Earth Sciences* 17, 405–418.
- Utkucu M. 2013: 23 October 2011 Van, Eastern Anatolia, earthquake (Mw7.1) and seismotectonics of Lake Van area. *J. Seismology* 12, 783–805.
- Üner S., Yeşilova Ç., Yakupoğlu T. & Üner T. 2010: Earthquake induced soft sediment deformation structures (seismites): Van Gölü Basin, Eastern Anatolia. [Pekişmemiş sedimanlarda depremlerle oluşan deformasyon yapıları (sismitler): Van Gölü Havzası, Doğu Anadolu]. *Yerbilimleri — Bulletin for Earth Sciences* 31, 1, 53–66 (in Turkish with English abstract).
- Valeton I. 1978: A morphological and petrological study of the terraces around Lake Van, Turkey. In: Degens E.T. & Kurtman F. (Eds.): The Geology of Lake Van. *Mineral Research and Exploration Institute Publication* 169, 64–80.
- Wise D.J., Cassidy J. & Locke C.A. 2003: Geophysical imaging of the Quaternary Wairoa North Fault, New Zealand: a case study. *Journal of Applied Geophysics* 53, 1–16.